Comparative analysis of phase extraction methods based on phase-stepping and shifting curve in grating interferometry*

Liu Xiao-Song(刘小松)[a], Li En-Rong(李恩荣)[a], Zhu Pei-Ping(朱佩平)[a)†], Liu Yi-Jin(刘宜晋)[a)b)], Zhang Kai(张 凯)[a], Wang Zhi-Li(王志立)[a], Hong You-Li(洪友丽)[a], Zhang Hui-Tao(张慧滔)[a)d)], Yuan Qing-Xi(袁清习)[a)], Huang Wan-Xia(黄万霞)[a)], and Wu Zi-Yu(吴自玉)[a)c)‡]

[a)] *Institute of High Energy Physics, Chinese Academy of Sciences, Beijing* 100049, *China*
[b)] *Department of Physics, University of Science and Technology of China, Hefei* 230026, *China*
[c)] *National Synchrotron Radiation Laboratory, University of Science and Technology of China, Hefei* 230029, *China*
[d)] *School of Mathematical Sciences, Capital Normal University, Beijing* 100048, *China*

(Received 1 April 2009; revised manuscript received 18 September 2009)

Two phase extraction methods which are based separately on phase-stepping and shifting curve are mainly used in phase-sensitive imaging in gating interferometry to determine the x-ray phase shift induced by an object in the beam. In this paper, the authors perform a full comparative analysis and present the main virtues and limitations of these two methods according to the theoretical analysis of the grating interferometry.

Keywords: x-ray phase sensitive imaging, grating interferometer, phase-stepping, shifting curve

PACC: 0785, 4280F, 8170J

1. Introduction

Hard x-ray phase sensitive imaging using a grating interferometer has been developed in recent years,[1−14] and it shows some excellent results.[4,13,15−17] This technique is based on Talbot self-imaging and can be used together with a broad bandwidth x-ray radiation generated by a conventional x-ray source.[5,7,13,15,18,19] Due to its compact setup and high sensitivity to weak-absorption materials such as soft tissue, polymer and so on, this technique has a potential biomedical application.

There are two main methods in grating interferometry to reveal the phase shift of an x-ray wave when it penetrates through an object. One is based on phase-stepping (PS) and the other on shifting curve (SC). The PS method,[2−5] which was first used in visible light interferometric imaging,[20] has widely been used in hard x-ray interferometry in these years. This method needs more than three images, from which three different signals can be extracted, namely the absorption image, the phase image and the dark-field image. The demand requirements of the PS method on alignment of the gratings and stability of the system are very low. On the other hand, the SC method[14] presented in 2008 needs only two images, and two kinds of signals, i.e. absorption image and phase image can be derived, and its requirements on alignment of the gratings and stability of the system are relatively high. In the present paper, the authors perform a full comparative analysis of these two methods, and present their main virtues and limitations.

2. Theory of grating interferometry

The grating interferometer, which is shown in Fig. 1, consists of two gratings with their lines parallel to each other. The first one is a phase grating

*Project supported by the Key Program of the National Natural Science Foundation of China (Grant Nos. 10490194 and 10734070), the National Natural Science Foundation of China (Grant Nos. 10504033, 10774144 and 10979055), the Knowledge Innovation Program of the Chinese Academy of Sciences (Grant No. KJCX2-YW-N42), the National Basic Research Program of China (Grant No. 2009CB930804) and the National Outstanding Youth Fund (Grant No. 10125523).
†Corresponding author. E-mail: zhupp@ihep.ac.cn
‡E-mail: wuzy@ihep.ac.cn, wuzy@ustc.edu.cn
© 2010 Chinese Physical Society and IOP Publishing Ltd

with a period of p_1 which is typically on the order of several micrometers, acting as a beam splitter that divides the incident coherent x-ray wave into beams of different diffraction orders. These diffracted beams would interfere with each other and form interference fringes with the period p at certain distances downstream of the phase grating, leading to a phenomenon known as the "fractional Talbot self-image effect".[21] The second one is an absorption grating with the same orientation and period as those of the fringes, acting as an analyzer and transforming the information about fringe shift into that of intensity varying on the detector plane. An area detector with a pixel size ranging from a few micrometers to a few tens of micrometers is located immediately at a distance downstream of the absorption grating.

When an object is arranged directly at a distance upstream of the phase grating, the incident x-ray will be deflected from the original direction due to refraction, and the refraction angle is proportional to the gradient of the phase shift of the x-ray wave induced by the object, which will cause a lateral displacement of the interference fringes in the self-image plane. Thus the intensity in the detector plane will change with the fringe displacement. A theoretical analysis will be given below.

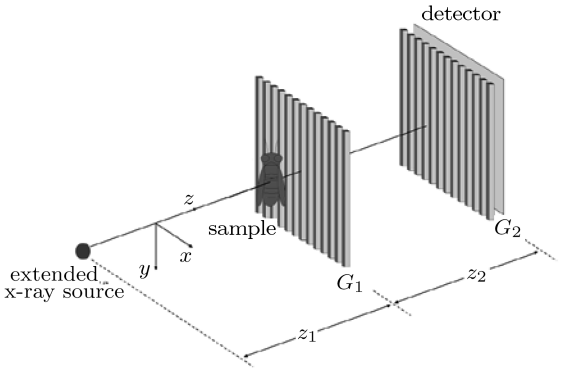


Fig. 1. Grating interferometer. G_1 is phase grating and G_2 is absorption grating. The object to be imaged is placed at a distance upstream of G_1 and the detector is at a distance downstream of G_2.

As shown in Fig. 1, the direction of the z-axis is parallel to the optical axis, and the x- and y-axes are both orthogonal to the z-axis, and the grating lines are parallel to the y-axis. In this work, the coordinate of y would be omitted because this technique requires no coherence of x-ray along the y-axis direction, and we take only one dimension of x into account for convenience. ς, x' and x are used to denote the coordinates of x-ray source, phase grating and self-image plane, respectively. The intensity distribution function of an extended x-ray source with the width w is $I_{\mathrm{s}}(\varsigma)$, and an object is set at the distance z_1 away from the x-ray source immediately followed by a phase grating. The complex transmission functions of the object and the phase grating are described by the following Eq. (1) and Eq. (2), respectively:

$$q\left(x'\right)=f\left(x'\right)\exp\left[\mathrm{i}\,\Phi\left(x'\right)\right], \tag{1}$$

where $f\left(x'\right)$ denotes the amplitude modulation and $\Phi\left(x'\right)$ the phase modulation of the object, and

$$t\left(x'\right)=\sum_n a_n\exp\left(\mathrm{i}\frac{2\pi}{p_1}nx'\right). \tag{2}$$

According to the theory of partial coherence, the intensity at the distance downstream of the phase grating, z_2, can be given by[22]

$$I(x)=\int\frac{1}{z_1}I_{\mathrm{s}}(\varsigma)\mathrm{d}\varsigma\iint\mu(x_1',x_2')q\left(x_1'\right)q^*\left(x_2'\right)t\left(x_1'\right)\times t^*\left(x_2'\right)\exp\left[\mathrm{i}\frac{2\pi}{\lambda}\left(r_1-r_2\right)\right]\Big/\lambda\sqrt{r_1r_2}\mathrm{d}x_1'\mathrm{d}x_2' \tag{3}$$

where

$$\mu\left(x_1',x_2'\right)=\frac{\exp\left(\mathrm{i}\Psi\right)\int I_{\mathrm{s}}\left(\varsigma\right)\exp\left[-\mathrm{i}\frac{2\pi}{\lambda z}\varsigma\left(x_1'-x_2'\right)\right]\mathrm{d}\varsigma}{\int I_{\mathrm{s}}\left(\varsigma\right)\mathrm{d}\varsigma}, \tag{4}$$

is the mutual coherence factor between the points x_1' and x_2' in the object plane, and $r_1=\sqrt{z_2^2+\left(x-x_1'\right)^2}$ and $r_2=\sqrt{z_2^2+\left(x-x_2'\right)^2}$ are the distances between x and x_1' and between x and x_2' respectively, with $\Psi=\pi\left(x'^2_1-x'^2_2\right)/\lambda z$ being the quadratic phase factor.

Substituting Eqs. (1), (2) and (4) into Eq. (3), in the paraxial approximation one obtains

$$I(x)=\int I_{\mathrm{s}}\left(\varsigma\right)u\left(x,\varsigma\right)u^*\left(x,\varsigma\right)\mathrm{d}\varsigma, \tag{5}$$

where

$$u(x,\varsigma)=\frac{1}{\sqrt{\lambda z_1z_2}}\exp\left(\mathrm{i}\frac{\pi}{\lambda z_1}\varsigma^2\right)\int f\left(x'\right)\exp\left[\mathrm{i}\Phi\left(x'\right)\right]\sum_n a_n\exp\left(\mathrm{i}\frac{2\pi}{p_1}nx'\right)\times\exp\left(\mathrm{i}\frac{\pi}{\lambda z_1}x'^2\right)\exp\left(-\mathrm{i}\frac{2\pi}{\lambda z_1}\varsigma x'\right)\exp\left[\mathrm{i}\frac{\pi}{\lambda z_2}\left(x-x'\right)^2\right]\mathrm{d}x', \tag{6}$$

is the wave field of the x-ray in the plane z_2, produced from an ideal point source at ς on the $z = 0$ plane.

In order to calculate the integral in Eq. (6), in each pixel we take $f(x')$ as a constant and use the first-order Taylor expansion of $\Phi(x')$ about the point $\frac{z_1}{z_1+z_2}\left(x+\frac{z_2}{z_1}\varsigma\right)$ (see Appendix) to approximate $\Phi(x')$ since it changes much more slowly than the complex transmission function $t(x')$:

$$\Phi(x') = \Phi\left[\frac{z_1}{z_1+z_2}\left(x+\frac{z_2}{z_1}\varsigma\right)\right] + \frac{2\pi}{\lambda}\left[x' - \frac{z_1}{z_1+z_2}\left(x+\frac{z_2}{z_1}\varsigma\right)\right]\varphi, \tag{7}$$

where

$$\varphi = \frac{\lambda}{2\pi}\frac{\partial\Phi}{\partial x'} \tag{8}$$

is the refraction angle induced by the object. For the hard x-ray grating interferometry, $1/\lambda z_2$ is a very large number, so the integral of Eq. (6) within one pixel (about several tens of microns) can be approximated as a Gaussian integral. Therefore $u(x,\varsigma)$ in Eq. (6) can be approximated as

$$\begin{aligned} u(x,\varsigma) \approx{}& \frac{1}{\sqrt{z_1+z_2}} f\left[\frac{z_1}{z_1+z_2}\left(x+\frac{z_2}{z_1}\varsigma\right)\right]\exp\left\{\mathrm{i}\Phi\left[\frac{z_1}{z_1+z_2}\left(x+\frac{z_2}{z_1}\varsigma\right)\right]\right\}\exp\left[\mathrm{i}\frac{\pi}{\lambda}\frac{(\varsigma-x)^2}{z_1+z_2}\right] \\ &\times\exp\left(-\mathrm{i}\frac{\pi}{\lambda}\frac{z_1z_2\varphi^2}{z_1+z_2}\right)\sum_n a_n\exp\left(-\mathrm{i}\pi\frac{\lambda z_1z_2}{z_1+z_2}\frac{n^2}{p_1^2}\right)\exp\left[\mathrm{i}\frac{2\pi}{p_1}\frac{z_1n}{z_1+z_2}\left(x+\frac{z_2}{z_1}\varsigma-z_2\varphi\right)\right]. \end{aligned} \tag{9}$$

Substituting Eq. (9) into Eq. (5), one obtains

$$I(x) = \int I_{\mathrm{s}}(\varsigma) I_{\mathrm{i}}\left(x+\frac{z_2}{z_1}\varsigma\right)\mathrm{d}\varsigma = I_{\mathrm{p}}(x) * I_{\mathrm{i}}(x), \tag{10}$$

where

$$I_{\mathrm{i}}(x) = \frac{1}{z_1+z_2} f^2\left(\frac{z_1x}{z_1+z_2}\right)\sum_n b_n\exp\left[\mathrm{i}\frac{2\pi}{p_1}\frac{z_1n}{z_1+z_2}(x-z_2\varphi)\right] \tag{11}$$

is the intensity in the z_2 plane, generated by an ideal x-ray point source at $\varsigma = 0$ on the $z = 0$ plane;

$$I_{\mathrm{p}}(x) = \frac{z_1}{z_2} I_{\mathrm{s}}\left(-\frac{z_2}{z_1}\varsigma\right) \tag{12}$$

is the point spread function of this imaging system, and it is also considered to be the pinhole image of the x-ray source in the z_2 plane;

$$b_n = \sum_{n_1-n_2=\eta n} a_{n_1}a_{n_2}^*\exp\left[-\mathrm{i}\pi\frac{\lambda z_1z_2}{z_1+z_2}\frac{\left(n_1^2-n_2^2\right)}{p_1^2}\right]. \tag{13}$$

When irradiated by a spherical x-ray wave, the fractional Talbot distances of the phase grating can be chosen as

$$z_2 = \frac{z_1z_{\mathrm{T}}}{z_1-z_{\mathrm{T}}}, \tag{14}$$

where

$$z_{\mathrm{T}} = m\frac{p_1^2}{2\eta^2\lambda}, \quad m = 1,3,\ldots, \tag{15}$$

are the fractional Talbot distances in the situation of plane x-ray wave illumination. The period of the interference fringes is

$$p = \frac{z_1+z_2}{z_1\eta}p_1, \tag{16}$$

where $\eta = 2$ if a π phase modulation grating is used and $\eta = 1$ if a $\pi/2$ phase modulation grating is adopted.[2,3,12]

Equation (10) indicates that the intensity in the Talbot self-image plane when illuminated by an extended x-ray source is the convolution of the interference intensity created by an ideal point x-ray source and a pinhole image of the extended x-ray source. If the width of the pinhole image w_{p} is smaller than p, there will still be interference fringes in the self-imaging plane.

The absorption grating whose period is identical to that of the interference pattern with the intensity transmission function

$$T(x) = \sum_n c_n\exp\left(\mathrm{i}\frac{2\pi}{p}nx\right), \tag{17}$$

is set to be in the fractional Talbot plane as a transmission mask. Scanning the lateral position x_{g} of one of the gratings (here the absorption grating), the transmitted intensity recorded by the detector with a pixel

size of several tens of micrometers is

$$I(X, x_{\rm g}) = \int I_{\rm s}(\varsigma) I_{\rm i}\left(X + \frac{z_2}{z_1}\varsigma, x_{\rm g}\right) {\rm d}\varsigma, \qquad (18)$$

where

$$I_{\rm i}(X, x_{\rm g}) = f^2\left(\frac{z_1}{z_1 + z_2}X\right) S_{\rm i}(x_{\rm g} + z_2\varphi) \qquad (19)$$

is the intensity generated by an ideal x-ray source at $\varsigma = 0$ in the detector plane, and

$$S_{\rm i}(x_{\rm g}) = \frac{1}{z_1 + z_2}\left[b_0 c_0 + \sum_{n\neq 0} b_n c_{-n} \times \exp\left(-{\rm i}\, 2\frac{\pi}{p} n x_{\rm g}\right)\right] \qquad (20)$$

is the intensity in the detector plane when illuminated by x-rays produced from an ideal point source without the sample in the beam.

As indicated by Eq. (20), $S_{\rm i}(x_{\rm g})$ is unrelated to the detector coordinate X and it reflects the relationship between the intensity of each pixel and the scanning position of the absorption grating. Therefore there will be intensity curves in each pixel when the absorption grating scans along the lateral direction with and without the objects in the beam, which are referred to as "shifting curves" whose expressions are given by Eq. (18). Equation (19) indicates that an object in the beam makes a lateral shift $z_2\varphi$ of the shifting curve.

Calculating the integral in Eq. (18), the expression of shifting curve can also be given by trigonometric series

$$I(X, x_{\rm g}) = f^2\left(\frac{z_1 X}{z_1 + z_2}\right) \times \sum_n \beta_n \cos\left[\frac{2\pi n}{p}(x_{\rm g} + z_2\varphi)\right], \qquad (21)$$

where β_n denotes the coefficient of the n-th order in the case of the extended x-ray source.

The shifting curve without object in the optical path is given by the following equation:

$$S_0(x_{\rm g}) = \sum_n \beta_n \cos\left(\frac{2\pi n}{p} x_{\rm g}\right). \qquad (22)$$

3. Methods to extract refraction angle in grating interferometry

Both the PS method and the SC method are based on detecting the refraction angle of the x-ray passing through a phase object.

3.1. Phase-stepping method

The PS method relies on the approximation that the shifting curve is a sinusoidal curve by keeping only the first term of the summation of Eq. (21), so that equation (21) can be rewritten as

$$I(X, x_{\rm g}) = f^2\left(\frac{z_1 X}{z_1 + z_2}\right) \times \left\{\beta_0 + \beta_1 \cos\left[\frac{2\pi}{p}(x_{\rm g} + z_2\varphi)\right]\right\}. \qquad (23)$$

An object upstream of the phase grating will cause a lateral displacement of the shifting curve in each pixel. When the absorption grating scans over one period along the x direction with and without objects in the beam, images are taken at each scanning position to determine the lateral shift of the shifting curves, and therefore the refraction angle induced by the object can be extracted by the following equation:[2,3]

$$\varphi = \frac{p}{2\pi z_2}\left\{\arg\left[\sum_{k=1}^{M} I^k \exp\left(-2\pi{\rm i}\frac{k}{M}\right)\right] - \arg\left[\sum_{k=1}^{M} I_0^k \exp\left(-2\pi{\rm i}\frac{k}{M}\right)\right]\right\}, \qquad (24)$$

where $M \geq 3$ is the number of scanning positions; I^k and I_0^k are the images acquired at the k-th scanning position with and without objects in the beam, respectively.

3.2. Shifting curve method

From Eqs. (21) and (22) it follows that the shifting curve with an object in the beam can be expressed as

$$I(X, x_{\rm g}) = f^2\left(\frac{z_1}{z_1 + z_2}X\right) S_0(x_{\rm g} + z_2\varphi). \qquad (25)$$

The shifting curve $S_0(x_{\rm g})$ without an object in the beam with a profile of a periodic sinusoidal-like curve as shown in Fig. 2 can be considered to be a reference shifting curve compared with that with an object in the beam.

Equation (25) has a similar form to the diffraction enhanced imaging (DEI) equation in Refs. [23]–[26]. Therefore, we can develop a similar method to extract refraction angle based on the shifting curve in grating interferometric imaging.[14]

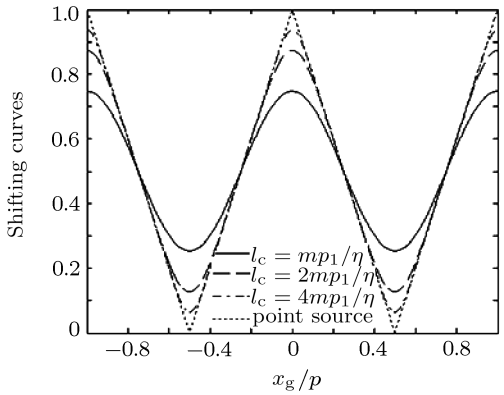


Fig. 2. Shifting curves of Gaussian x-ray with three different coherence lengths, i.e. $l_c = mp_1/\eta$ (solid line), $l_c = 2mp_1/\eta$ (dash line), and $l_c = 4mp_1/\eta$ (dash-dot line) in the m-th self-image plane. The dot line is the shifting curve of an ideal point source for which $l_c \to +\infty$.

The slopes of the shifting curves are steepest at the scanning points where the values of the shifting curves are equal to half the sum of maximum and minimum which is referred to as "half slopes", and small $z_2\varphi$ can cause observable change in intensity at these positions.

In order to acquire the phase signal of an object, we need to take images at both left and right half slopes of the reference shifting curve over one period. As there are large ranges of linearity in the vicinity of these half slopes, the values of the shifting curve at $-x_g/4 + z_2\varphi$ and $x_g/4 + z_2\varphi$ with $\varphi < p/4z_2$ can be replaced with the corresponding first order Taylor expansion, and therefore the refraction angle can be extracted from the left-slope image and the right-slope image by using the following equation:[14]

$$\varphi = \frac{1}{z_2} \frac{I_L\left(X, -\frac{p}{4}\right) S_0\left(\frac{p}{4}\right) - I_R\left(X, \frac{p}{4}\right) S_0\left(-\frac{p}{4}\right)}{I_L\left(X, -\frac{p}{4}\right) \frac{dS_0}{dx_g}\left(\frac{p}{4}\right) - I_R\left(X, \frac{p}{4}\right) \frac{dS_0}{dx_g}\left(-\frac{p}{4}\right)}, \tag{26}$$

where I_L and I_R denote the intensity of the left- and right-slope images, respectively.

4. Comparative analysis of these two methods to extract refraction angle

4.1. The x-ray doses

The PS method requires collecting three or more images at different scanning positions of the absorption grating while the SC method requires only two images taken at the left and right half-slopes. The x-ray dose delivered to the object in the PS method is $M/2$ times more than that in the SC method.

4.2. Alignment and stability

The issue of alignment concerns the parallelisms of the planes and the lines of the gratings. The former is easily solved and not a problem considered in grating interferometry, and the latter is referred to as angular alignment.

In the PS method, the angular misalignment θ of these two gratings about the optical axis which will cause the moiré fringe to exert no significant effect on the extraction of refraction angle with $\theta \ll 1$, since the effect of moiré fringes in the image will cancel out in the subtraction of the background image.

The mechanical stability of one grating relative to the other is required to be reduced down to a length-scale of approximately one-tenth of the period p, and the same length-scale is also required for the accuracy of the transverse grating motion used in the PS method.[3]

Nonetheless, for the SC method, the two gratings must be well aligned since it requires collecting images with the absorption grating tuned to two positions which correspond to the half slopes of the shifting curves of all the object pixels, and the angular misalignment θ must not exceed $p/4Y$, where Y is the width of the field of view in the direction along the grating lines.

4.3. Qualities of refraction image

The PS method, which calculates the refraction angle by measuring the displacement of the shifting curves, is not sensitive to the refraction angle φ that is much smaller than $p/4z_2$ because the shifting curve is determined from the M images over one scanning period by sine curve fitting. The refractive angle within a range of $(-p/2z_2,\ p/2z_2)$ can be directly extracted

from Eq. (24), while the angle out of $(-p/2z_2,\ p/2z_2)$ can be obtained through an additional phase unwrapping algorithm.

On the other hand, as the images are always taken at half slopes of the reference shifting curves in the SC method, even a small refraction angle can cause observable intensity change because of the steep slopes, which makes the SC method very sensitive to the angle within the linearity range in the vicinity of the half slopes. If the refractive angle is out of the linearity range but within a range of $(-p/4z_2,\ p/4z_2)$, equation (26) may give a result with some tolerable error due to the first Taylor approximation of the shifting curve. If the refraction angle is out of the range $(-p/4z_2,\ p/4z_2)$, however, equation (26) may give a qualitative result.

4.4. Requirement for coherence

To ensure a considerable visibility of the interference fringes in the m-th self-image plane, the width of the pinhole image of the extended source in the m-th self-image plane $w_{\rm p}$ must not be larger than $p/2$, i.e. the lateral coherence length of the incident x-ray $l_{\rm c}$ must satisfy the condition

$$l_{\rm c} \geq \frac{m}{\eta} p_1. \tag{27}$$

In the PS method the shifting curve is assumed to be sinusoidal, so other terms (higher orders) except the first one of the summation in Eq. (21) may induce errors in the result. The higher orders except those corresponding to $n = 1 \pm qM$, where q is a nonzero integer, will not contribute to the result since the summation in Eq. (24) of each of these terms returns to zero.[4] Also, the effects of the terms corresponding to $n = 1 \pm qM$ can be cancelled when the coherence length $l_{\rm c}$ of the incident x-ray is limited by

$$l_{\rm c} \leq \frac{nm}{2\eta} p_1. \tag{28}$$

The SC method relies mainly on the magnitude of the slope at and the linearity range in the vicinity of the half slopes of the shifting curve, which are determined by the coherence length of the incident x-ray wave.

Figure 2 shows the shifting curves for incident x-rays with different coherence lengths. As shown in Fig. 2, the larger the coherence length of the incident x-ray is, the larger the magnitude of the slope and the linearity range will be, which means that it is more sensitive to refraction angle. However, when the coherence length is larger than $4mp_1/\eta$, the increase in coherence length does not result in significant change in the slope and the mentioned linearity range.

5. Conclusion

A complete comparative analysis of two methods to extract the refraction angle in grating interferometric imaging, namely the PS method and the SC method, is given in this paper. The former requires the collection of three or more images at different scanning positions of the absorption grating and can work with a poorly aligned setup and an unstable system but insensitively to angles much smaller than $p/4z_2$. On the other hand, the latter requires only two images and thus reduces the dose delivered to the sample which is a key advantage for biomedical application even though it strongly requires the perfection and strict alignment of the two gratings and the stability of the imaging system. Meanwhile, it is sensitive to even a very small angle and it is thus able to reveal fine structures.

Appendix

The summation of

$$\sum_n a_n \exp\left(\mathrm{i}\frac{2\pi}{p_1} n x'\right) \exp\left(\mathrm{i}\frac{\pi}{\lambda z_1} x'^2\right) \exp\left(-\mathrm{i}\frac{2\pi}{\lambda z_1} \varsigma x'\right) \exp\left[\mathrm{i}\frac{\pi}{\lambda z_2} (x - x')^2\right] \tag{A1}$$

in Eq. (6) can be rewritten as

$$\begin{aligned} &\exp\left\{\mathrm{i}\frac{2\pi}{\lambda}\left[\frac{x^2}{2z_2} - \frac{z_1 z_2}{2(z_1+z_2)}\left(\frac{\varsigma^2}{z_1^2} + \frac{x^2}{z_2^2} + 2\frac{\varsigma x}{z_1 z_2}\right)\right]\right\} \\ &\times \sum_n a_n \exp\left(\mathrm{i}\frac{2\pi}{p_1} n x'\right) \exp\left\{\mathrm{i}\frac{\pi}{\lambda}\frac{z_1+z_2}{z_1 z_2}\left[x' - \frac{z_1 z_2}{z_1+z_2}\left(\frac{x}{z_2} + \frac{\varsigma}{z_1}\right)\right]^2\right\}. \end{aligned} \tag{A2}$$

The first term in expression (A2) does not contain x', so it can be moved out of the integral sign in Eq. (6), meanwhile the third term explicates the Fresnel integral of Eq. (6), suggesting that $\Phi(x')$ can be expanded in the vicinity of $[z_1/(z_1+z_2)][x+(z_2/z_1)\varsigma]$.

References

[1] David C, Nohammer B, Solak H H and Ziegler E 2002 *Appl. Phys. Lett.* **81** 3287

[2] Momose A, Kawamoto S, Koyama I, Hamaishi, Y, Takai K and Suzuki Y 2003 *Jpn. J. Appl. Phys.* Part 2: *Lett.* **42** L866

[3] Weitkamp T, Diaz A, David C, Pfeiffer F, Stampanoni M, Cloetens P and Ziegler E 2005 *Opt. Express* **13** 6296

[4] Momose A, Yashiro W, Takeda Y, Suzuki Y and Hattori T 2006 *Jpn. J. Appl. Phys.* Part 1: *Regular Papers, Brief Communications & Review Papers* **45** 5254

[5] Pfeiffer F, Weitkamp T, Bunk O and David C 2006 *Nature Phys.* **2** 258

[6] David C, Weitkamp T, Pfeiffer F, Diaz A, Bruder J, Rohbeck T, Groso A, Bunk O, Stampanoni M and Cloetens P 2007 *Spectrochimica Acta Part B-Atomic Spectroscopy* **62** 626

[7] Engelhardt M, Baumann J, Schuster M, Kottler C, Pfeiffer F, Bunk O and David C 2007 *Appl. Phys. Lett.* **90** 224101

[8] Kottler C, David C, Pfeiffer F and Bunk O 2007 *Opt. Express* **15** 1175

[9] Liu X, Guo J C, Peng X and Niu H B 2007 *Chin. Phys.* **16** 1632

[10] Takeda Y, Yashiro W, Suzuki Y, Aoki S, Hattori T and Momose A 2007 *Jpn. J. Appl. Phys.* Part 2: *Lett.* & *Express Lett.* **46** L89

[11] Jiang M, Wyatt C L and Wang G 2008 *J. Biomedic. Imag.* **2008** 1

[12] Nesterets Y I and Wilkins S W 2008 *Opt. Express* **16** 5849

[13] Pfeiffer F, Bech M, Bunk O, Kraft P, Eikenberry E F, Bronnimann C, Grunzweig C and David C 2008 *Nature Mater.* **7** 134

[14] Chen B, Zhu P P, Liu Y J, Wang J Y, Yuan Q X, Huang W X, Ming H and Wu Z Y 2008 *Acta Phys. Sin.* **57** 1576 (in Chinese)

[15] Kottler C, Pfeiffer F, Bunk O, Grunzweig C, Bruder J, Kaufmann R, Tlustos L, Walt H, Briod I, Weitkamp T and David C 2007 *Phys. Status Soli.* **204** 2728

[16] Pfeiffer F, Bunk O, David C, Bech M, Duc G L, Bravin A and Cloetens P 2007 *Physics in Medicine and Biology* **52** 6923

[17] Weitkamp T, David C, Bunk O, Bruder J, Cloetens P and Pfeiffer F 2008 *Euro. J. Radiol.* **68** S13

[18] Pfeiffer F, Kottler C, Bunk O and David C 2007 *Phys. Rev. Lett.* **98** 8105

[19] Donath T, Pfeiffer F, Bunk O, Groot W, Bednarzik M, Grunzweig C, Hempel E, Popescu S, Hoheisel M and David C 2008 *Developments in X-Ray Tomography VI* **7078** 707817

[20] Bruning J H, Herriott D R, Gallagher J E, Rosenfeld D P, White A D and Brangaccio D J 1974 *Appl. Opt.* **13** 2693

[21] Cloetens P, Guigay J P, DeMartino C, Baruchel J, and Schlenker M 1997 *Opt. Lett.* **22** 1059

[22] Born M and Wolf E 1999 *Principles of Optics* 7$^{\text{th}}$ ed. (New York: Cambridge University Press) p. 562

[23] Chapman D, Thomlinson W, Johnston R E, Washburn D, Pisano E, Gmur N, Zhong Z, Menk R, Arfelli F and Sayers D 1997 *Physics in Medicine and Biology* **42** 2015

[24] Huang W X, Yuan Q X, Tian Y L, Zhu P P, Jiang X M and Wang J Y 2005 *Acta Phys. Sin.* **54** 677 (in Chinese)

[25] Zhu P P, Yuan Q X, Huang W X, Wang J Y, Shu H, Wu Z Y and Xian D C 2006 *Acta Phys. Sin.* **55** 1089 (in Chinese)

[26] Zhu P P, Yuan Q X, Huang W X, Wang J Y, Shu H, Chen B, Liu Y J, Li E R and Wu Z Y 2006 *J. Phys.* D: *Appl. Phys.* **39** 4142